
Published paper

Wallin, A.E., Ojala, H., Haeggstrom, E. and Tuma, R. (2008) *Stiffer optical tweezers through real-time feedback control,* Applied Physics Letters, Volume 92 (22), 224104.

Stiffer optical tweezers through real-time feedback control

Anders E Wallin, Heikki Ojala, and Edward Hæggström

Department of Physics, P.O.Box 64, 00014, University of Helsinki, Finland

Roman Tuma

Institute of Biotechnology, University of Helsinki, Finland, and

Astbury Centre for Structural Molecular Biology, University of Leeds, LS29JT United Kingdom

Using real-time re-programmable signal processing we connect acousto-optic steering and back-focal-plane interferometric position detection in optical tweezers to create a fast feedback controlled instrument. When trapping 3 μm latex beads in water we find that proportional-gain position-clamping increases the effective lateral trap stiffness ~13-fold. A theoretical power-spectrum for bead fluctuations during position-clamped trapping is derived and agrees with the experimental data. The loop-delay, ~19 μs in our experiment, limits the maximum achievable effective trap stiffness.

87.80.Cc (optical trapping), 87.85.ff (feedback)

Feedback control has been employed at the nanoscale to confine single molecules in fluorescence studies[1,2], to maintain constant force or torque in optical tweezers experiments[3,4], and to control atomic force microscope tips[5]. A constant-tension assay is indispensable in the study of molecular motor mechanisms and has traditionally been achieved by analog circuitry [6] or slow stage-based control [7,8].

Few reports on the real-time position-clamp control of optically trapped particles have been published. Simmons *et al.* [6] reported a 400-fold improvement in trap stiffness using feedback control, while simulations by Ranaweera *et al.* [9] using nonlinear control estimated the achievable stiffness increase to be 65-fold. Wulff *et al.* [10] used steering mirrors for feedback control, and were able to reduce the low-frequency (<100 Hz) fluctuations. However, Wulff *et al.* used the trapping beam for position-detection, potentially contaminating the position detection signal with cross-talk from steering.

We provide an experimental and theoretical description of proportional-gain feedback controlled optical tweezers. We control the position of an optical trap in real-time based on position detection signals from a stationary detection laser. An independent out-of-loop detection laser provides an unbiased verification of bead position.

Our optical tweezers are built on an air-damped table around an inverted microscope (Fig. 1). A 1064 nm 4 W continuous wave trap laser is first collimated with a 1:1 telescope (L1:L2) and optically isolated with a Faraday isolator (FI). The beam is steered using two orthogonal acousto optic deflectors (AOD). A second (1:3, L3:L4) and third

(1:1, L5:L6) telescope expand the beam to overfill the back aperture of a 100x 1.2 numerical aperture (NA) objective (OBJ). The back-aperture of the objective is imaged onto a plane between the AODs. Rotating the beam around a point on the optical axis between the AODs translates the focal spot in the sample plane [11]. The AODs provide a maximum deflection of ±16 mrad which corresponds to ±11 μm trap translation. Direct digital synthesizers (DDS) with 30-bit control words drive the AODs with a resolution of 0.02 pm in the sample plane. The trapping beam enters the microscope light-path through dichroic D2.

To track microsphere position we use two independent detection channels in the back-focal-plane interferometric configuration [12]. Temperature-stabilized optically isolated diode lasers at 830 nm and 785 nm were chosen to achieve high bandwidth using Si detectors [13,14]. Beam quality and pointing stability is improved by single-mode fiber (SMF) coupling. The detection beams are combined with a polarizing beam-splitter (PBS1), expanded (1:2, L7:L8), and combined with the trapping beam using dichroic D1.

To achieve high spatial resolution in the transverse direction a 1.4 NA condenser (COND) collects light scattered by trapped objects [15]. The back-focal-plane of the condenser is imaged onto two 2D position sensitive detectors (PD1/2) using L9. Cross-talk between the detection channels is eliminated with a polarizing beam splitter (PBS2) in combination with laser-line filters (F1/2). Variable gain instrumentation amplifiers match the position detection signal amplitude to the ±10 V input range of the analog to digital (AD) converter.

Data collection, real-time control, and trap steering is performed with a data acquisition card incorporating a 3 million gate field programmable gate array (FPGA, model PCI-7833R, National Instruments). The FPGA-card, programmed using LabVIEW 8.5, allows control algorithms to run in real-time (200 kHz loop rate) independently of the host operating system and other computer peripherals.

Analog voltages, corresponding to the bead position measured independently with 830 nm and 785 nm laser beams, are digitized at 200 kS/s with 16-bit precision. A proportional-gain position-clamping algorithm, Eq. (3), is run every 5 μs. Based on the 785 nm detection signals two 30-bit control words are output to the DDSs that drive the AODs. The 830 nm detection signals serve as an independent out-of-loop bead position measurement, since in-loop detection may introduce bias [16].

The power spectral density (PSD) of bead position fluctuations is widely used to characterize optical trapping. A stationary harmonic trap results in a Lorentzian PSD [17]. However, during feedback control the trap position fluctuates and the PSD becomes non-Lorentzian. The Langevin equation (ignoring inertia) for a bead trapped by steerable optical tweezers is

$$\beta\,\dot{x}(t) + k\big(x(t) - x_{trap}(t)\big) = F_T(t) \ , \tag{1}$$

where β is the drag-coefficient, k the trap stiffness, x the bead position, and x_{trap} the trap position. F_T is a thermal noise term with zero mean and a constant PSD of $\left|\tilde{F}_T(f)\right|^2 = 4k_B T\beta$. In proportional-gain feedback control the trap is steered so that

$$x_{trap}(t) = K_p\left(x_{set} - x(t-\tau)\right) \ , \tag{2}$$

where x_{set} is the loop set-point, K_p is the feedback gain, and τ accounts for a delay in position measurement and trap steering. Inserting Eq. (2) into Eq. (1) the PSD for a proportional-gain position-clamped bead with $x_{set} = 0$ can be obtained:

$$\left|\tilde{x}(f)\right|^2 = \frac{4k_BT\beta}{\left|i2\pi f\beta + kK_p\exp(-i2\pi f\tau) + k\right|^2} \ . \tag{3}$$

This PSD exhibits a resonance peak at $f \approx 1/(4\tau)$ when K_p is high, but reduces to the Lorentzian form when feedback control is switched off, *i.e.* $K_p = 0$. Using the equipartition theorem we define the effective trap stiffness

$$k_{eff} = \frac{k_BT}{<x^2>} \ , \tag{4}$$

which is used to characterize our position-clamp. Here $<x^2>$ may be determined directly from an observed time-series, from the PSD through Parseval's theorem, or, if the trap is harmonic, by fitting a Gaussian to the position histogram.

The instrument was calibrated at zero gain as described in [18]. Latex beads (3 µm diameter, Micromod) were trapped with a constant trapping laser power (500 mW) in water at room temperature. Both detection lasers were focused to the same point, and a trapped bead was centered in the detection area. Bead and trap position data was then recorded while the feedback gain was increased from $K_p = 0$ to $K_p = 24.8$, after which trapping became unstable. Signals from the 785 nm laser (not shown) were used for feedback control, while the independent out-of-loop data from the 830 nm laser was analyzed. Bead position histograms and PSDs for representative K_p values are shown in

Fig. 2 and 3. Each of the histograms is well approximated by a single Gaussian. The fits indicate that the effective trap stiffness increases from 26 pN/μm at $K_p = 0$ to a maximum of 340 pN/μm at $K_p = 16$. The PSD at zero gain shows a Lorentzian shape (Fig 3). In agreement with the prediction of a resonance at $f \approx 1/(4\tau)$, a peak at ~12 kHz appears at high gains. To compare the theoretical PSD, Eq. (3), to the experimental data we first determined β and k from a fit to the zero-gain PSD and then estimated $\tau \approx 19$ μs from a fit to the data with the highest gain. Theoretical PSDs for $0 < K_p < 24.8$ were then plotted, without free parameters, and agree well with experimental PSDs (Fig. 3, solid lines). Finally we determined k_{eff} as a function of K_p from the histogram fits, and alternatively by integrating the PSDs (Fig. 3, inset). A comparison to a prediction obtained by numerically integrating Eq. (3) shows good agreement with theory. At $K_p >$ ~10 the PSD becomes increasingly non-Lorentzian and thus the trap non-harmonic, which accounts for the slight difference observed between calculating k_{eff} from a position histogram (which assumes a linear trap) and calculating k_{eff} by finding $< x^2 >$ from the time-series or the PSD.

This letter shows that position-clamping a 3 μm latex bead in water can increase the effective lateral trap stiffness ~13-fold. Instability due to finite loop-delay and the associated resonance peak in the PSD limits the maximum loop gain. The AD conversion time (5 μs) and the acoustic time-of-flight in the AOD (10 μs) explain most of the observed 19 μs loop-delay. We also provide an expression for the PSD of a position-clamped bead, Eq. (3), which agrees well with experiments (Fig. 3). This PSD can be used to predict the effect of feedback control in experiments where the loop-delay and the open-loop trap stiffness are known. Feedback control of optical tweezers using a position-clamp algorithm provides, at constant laser power, an effective lateral trap stiffness several times the value achieved without feedback. Using less laser power to achieve a stiff trap reduces optical damage to specimens [19] and may also reduce photo-bleaching in instruments that combine tweezers with fluorescence [20]. In particular, real-time position-clamps may find use in trapping and controlling small (<100 nm) metal particles or other hard-to-trap objects [21]. Our real-time hardware and software can easily be adapted for other time-sensitive trapping experiments such as force-clamping, time-sharing of multiple traps, or possibly noise- and trap potential-shaping.

This work was supported by the Finnish Centre of Excellence in Virus Research 2006-2011 (grant nr.213467), the Academy of Finland (grant nr. 118462 to R.T.), and University of Helsinki HENAKOTO funding to E.H. A.E.W is supported by the Finnish National Graduate School of Nanosciences and the Jenny and Antti Wihuri Foundation.

[1] A.J. Berglund, K. McHale, and H. Mabuchi, Opt. Lett. **32** (2), 145-147 (2007).

[2] A.E. Cohen and W.E. Moerner, Proc. Natl. Acad. Sci. USA. **103** (12), 4362-4365 (2006).

[3] S. M. Block, C.L. Asbury, J. W. Shaevitz, and M.J. Lang, Proc. Natl. Acad. Sci. USA. **100** (5), 2351-2356 (2003).

[4] T. Pilizota, T. Bilyard, F. Bai, M. Futai, H. Hosokawa, and R.M. Berry, Biophys. J. **93**, 264-275 (2007).

[5] N. Kodera, M. Skashita, and T. Ando, Rev. Sci. Instrum. **77**, 083704 (2006).

[6] R. M. Simmons, J.T. Finer, S. Chu, and J. A. Spudich, Biophys. J. **70**, 1813-1822 (1996).

[7] G. J. Wuite, R. J. Davenport, A. Rappaport, and C. Bustamante, Biophys J **79** (2), 1155-1167 (2000).

[8] M.J. Lang, C.L. Asbury, J. W. Shaevitz, and S. M. Block, Biophys. J. **83**, 491-501 (2002).

[9] A. Ranaweera and B. Bamieh, Int. J. Robust. Nonlin. **15**, 747-768 (2005).

[10] K.D. Wulff, D.G. Cole, and R.L. Clark, Appl. Opt. **46**, 4923-4931 (2007).

[11] E Fällman and O Axner, Appl. Opt. **36** (10), 2107-2113 (1997).

[12] F. Gittes and C.F. Schmidt, Opt. Lett. **23** (1), 7-9 (1998).

[13] K Berg-Sorensen, L Oddershede, E-L Florin, and H Flyvbjerg, J. Appl. Phys. **93** (6), 3167-3176 (2003).

[14] J Huisstede, B van Rooije, K van der Werf, M Bennink, and V Subramaniam, Opt. Lett. **31** (5), 610-612 (2006).

[15]A. Rohrbach, H. Kress, and E.H.K Stelzer, Opt. Lett. **28** (6), 411-413 (2003).

[16]A.R. Carter, G.M King, T.A. Ulrich, W Halsey, D Alchenberger, and T. T. Perkins, Appl. Opt. **46** (3), 421-427 (2006).

[17]K Berg-Sorensen and H Flyvbjerg, Rev. Sci. Instrum. **75** (3), 594-612 (2004).

[18]A.E. Wallin, H. Ojala, A Korsbäck, E. Haeggström, and R. Tuma, Proc. SPIE **6644**, 66441Y (2007).

[19]E.J.G. Peterman, F. Gittes, and C.F. Schmidt, Biophys. J. **84**, 1308-1316 (2003).

[20]M.J. Lang, P.M. Fordyce, A.M. Engh, K. C. Neuman, and S. M. Block, Nature Methods **1**, 133-139 (2004).

[21]Y. Seol, A.E. Carpenter, and T. T. Perkins, Opt. Lett. **31** (16), 2429-2431 (2006).

FIG. 1. (Color online) Optical and electronic setup. Components inside the dotted line are mounted inside or on the inverted microscope. Dashed lines show planes conjugate to the back-focal-plane (BFP) of the objective. TL = Tube Lens, M = Dielectric Mirror, DA = Digital to analog converter, CCD = Camera.

FIG 2. (Color online) Normalized bead position histograms (symbols) with Gaussian fits to data (lines).

FIG. 3. (Color online) Bead position PSD data for increasing feedback gain. The theoretical PSDs, Eq. (3), are shown as solid lines. (inset) Effective trap stiffness as a function of feedback gain. Filled and open symbols show k_{eff} determined from Gaussian histogram fits and calculated from the PSD, respectively. The solid line shows a prediction from Eq. (3) and Eq. (4).

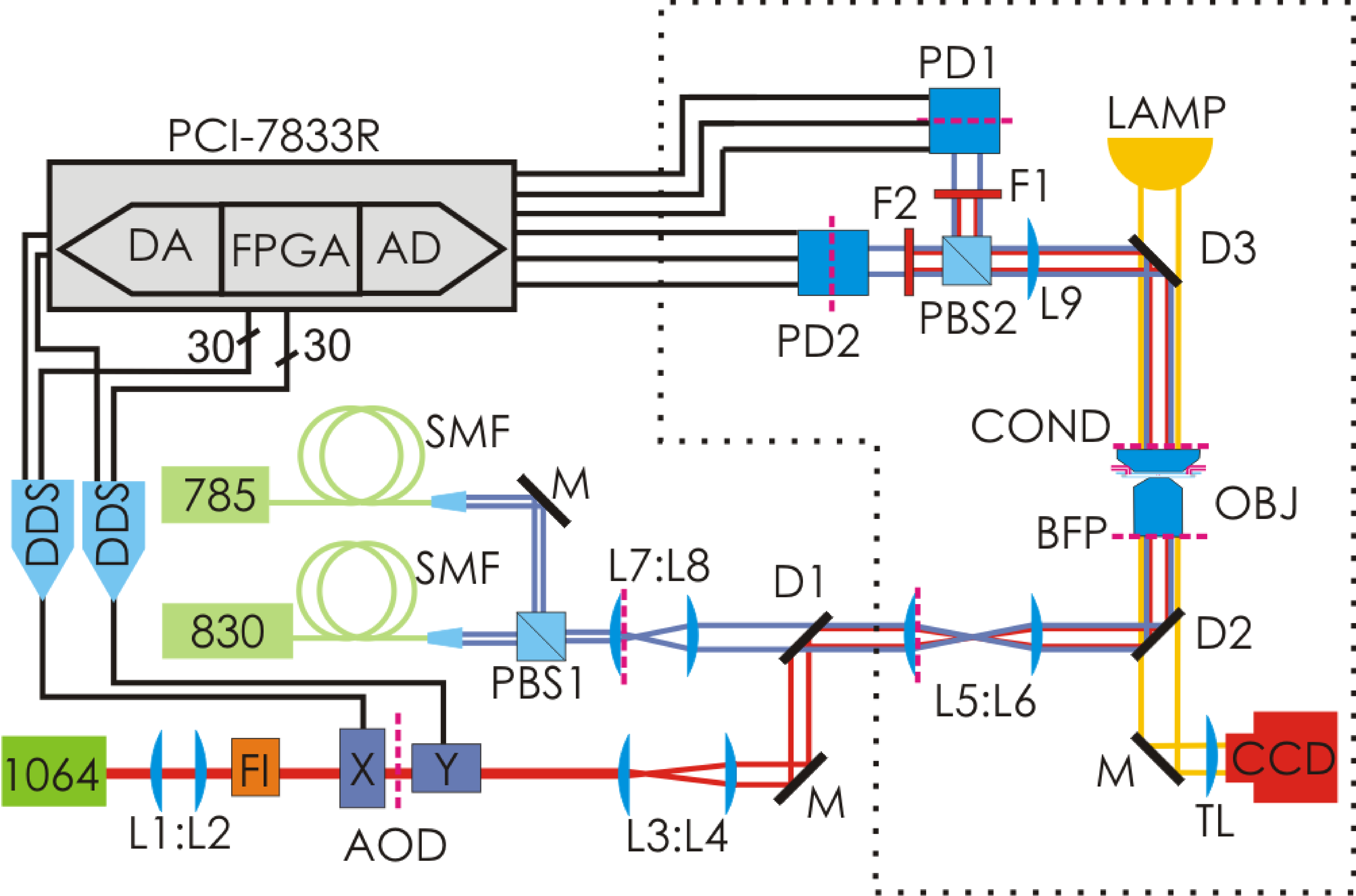
PD1
PCI-7833R
LAMP
F1
F2
DA
FPGA
AD
D3
PD2
PBS2
L9
30
30
COND
SMF
785
M
OBJ
BFP
SMF
L7:L8
D1
830
PBS1
D2
L5:L6
DDS
DDS
CCD
1064
FI
X
Y
M
M
TL
L1:L2
AOD
L3:L4

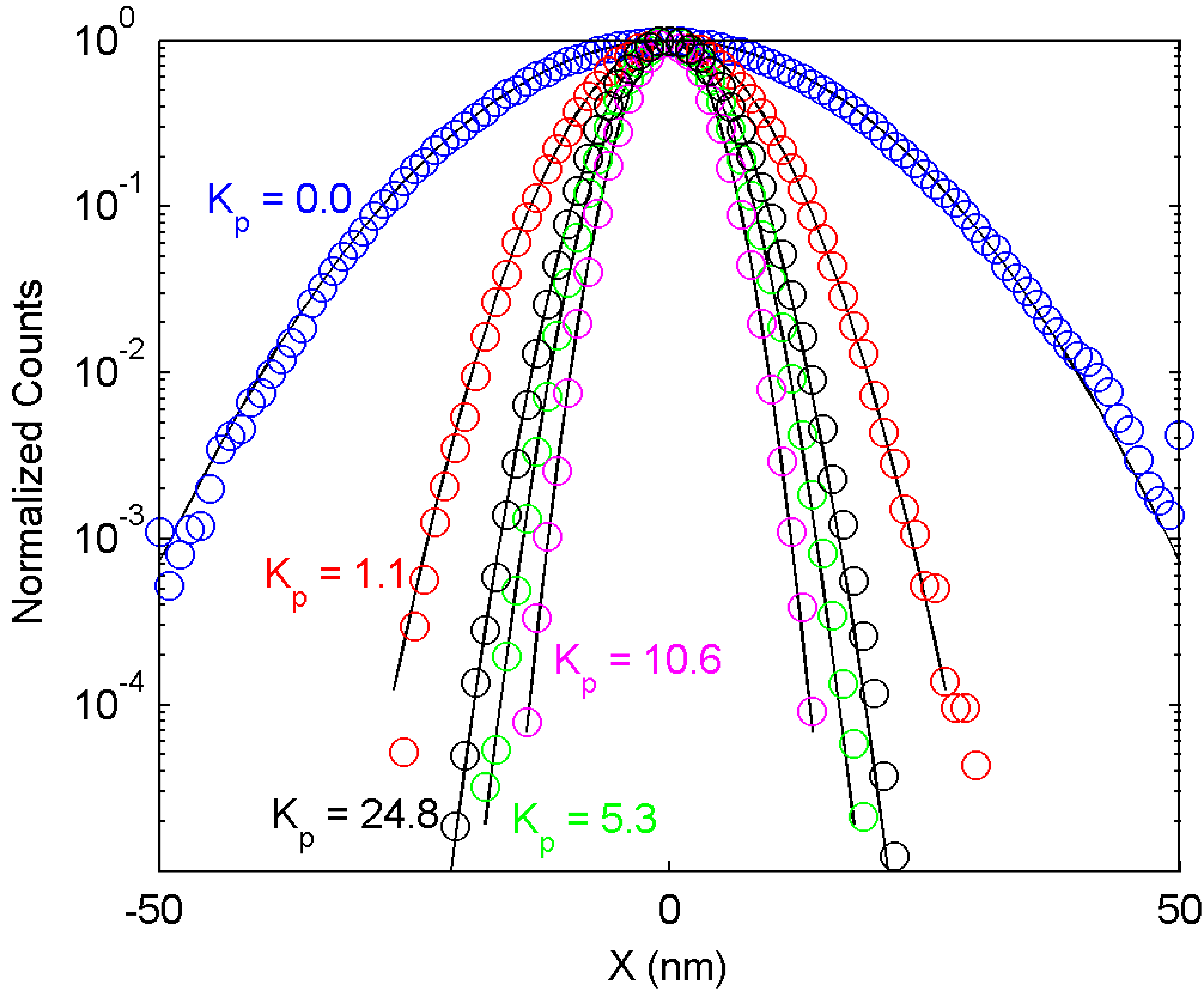

10^0
10^{-1}
10^{-2}
10^{-3}
10^{-4}
Normalized Counts
$K_p = 0.0$
$K_p = 1.1$
$K_p = 10.6$
$K_p = 24.8$
$K_p = 5.3$
-50
0
50
X (nm)

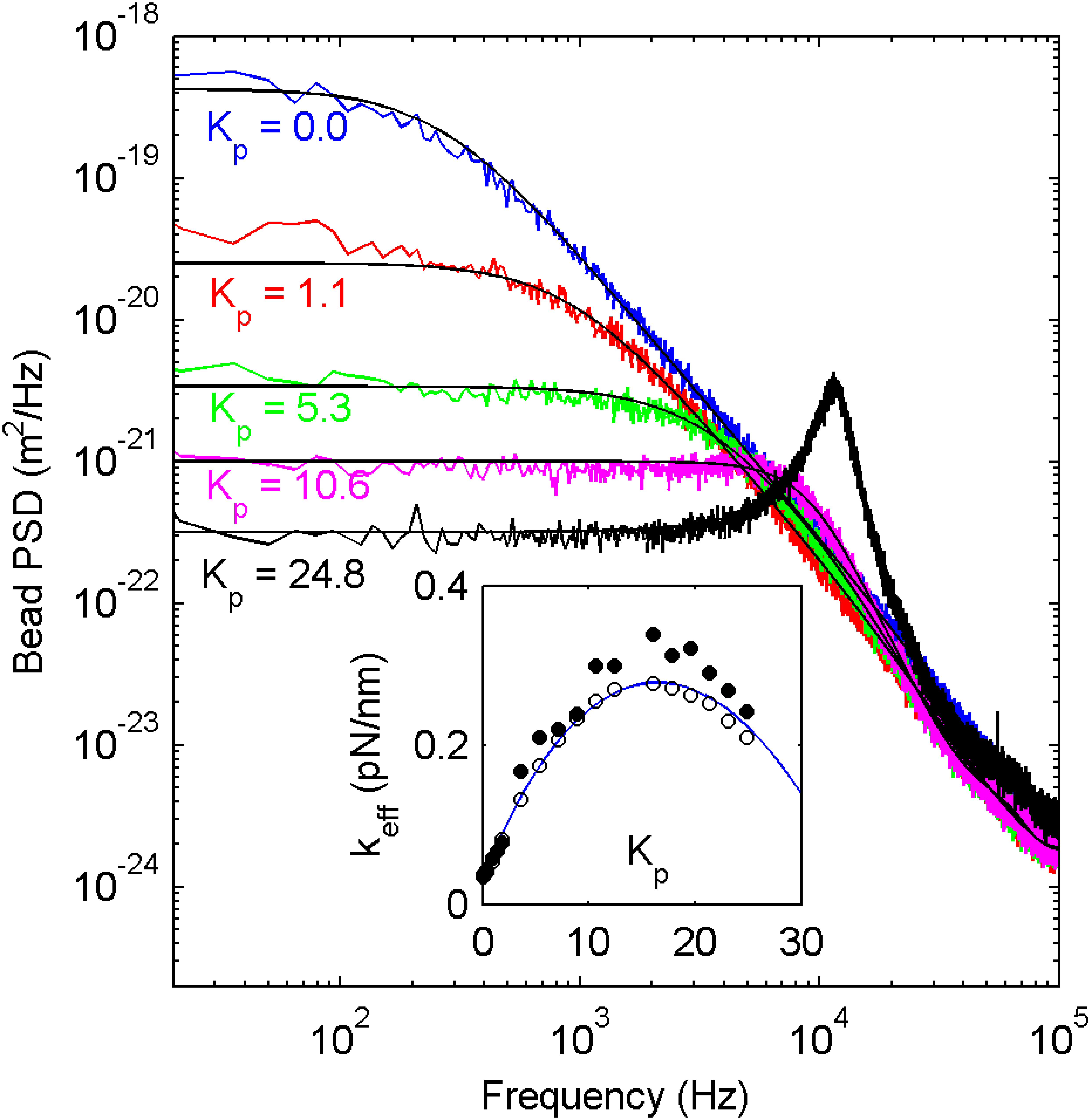
Bead PSD (m^2/Hz)
10^{-18}
10^{-19}
10^{-20}
10^{-21}
10^{-22}
10^{-23}
10^{-24}
K_p = 0.0
K_p = 1.1
K_p = 5.3
K_p = 10.6
K_p = 24.8
Frequency (Hz)
10^2
10^3
10^4
10^5
k_{eff} (pN/nm)
0.4
0.2
0
K_p
0
10
20
30